ChemComm

ROYAL SOCIETY OF CHEMISTRY

COMMUNICATION

View Article Online
View Journal | View Issue

Check for updates

Cite this: *Chem. Commun.*, 2021, **57**, 5082

Received 6th March 2021,
Accepted 13th April 2021

DOI: 10.1039/d1cc01229k

rsc.li/chemcomm

Published on 13 April 2021. Downloaded on 4/5/2026 1:25:58 AM.

Mechanochromic properties in a mononuclear Cu(I) complex without cuprophilic interactions†

Xiao Yu,[a] Xiaoyue Li,[b] Zelun Cai,[b] Lingzhi Sun,[a] Chengbo Wang,[b] Haixia Rao,[b] Chen Wei,[b] Zuqiang Bian,[b] Qionghua Jin*[a] and Zhiwei Liu*[b]

Two polymorphs of Cu[(3,4-bis(diphenylphosphino)thiophene)(bis(pyrazol-1-yl)borohydrate)] (1) were isolated. The blue luminescent crystals have evident mechanochromic luminescent (MCL) properties. Based on photophysical and structural analysis, the pore structure in the blue crystals is considered to be the main reason for the MCL properties.

During the past decade, stimuli-responsive materials have been extensively investigated due to the soaring demand for efficient smart materials.[1] Thus far, a number of stimuli-responsive molecules have been synthesized, and they are sensitive to diverse external stimulations.[2] Mechanochromic luminescent (MCL) material that can exhibit color changes in response to external mechanical stimulations (*e.g.*, grinding, shearing, or high pressure) is an attractive research target, due to the numerous promising applications for it, from sensing to data storage and displays.[3] However, these types of materials are still limited, and a significant number of MCL molecules have been discovered serendipitously or as a result of deliberate screening.[4] Moreover, compared with π-conjugated organic molecules, transition-metal complexes are less studied, and they are mainly based on noble metals such as Au(I).[5] In addition, because direct identification of the ground amorphous phase is usually absent, the understanding of mechanochromic mechanisms remains in its infancy.

There has been great interest in Cu(I) complexes in recent years because of their relatively low cost, structural diversity, and outstanding photophysical behaviors.[6] Stimuli-responsive materials based on Cu(I) complexes were studied as early as the 1970s, but the report on Cu(I) complex-based MCL material did not appear until decades later.[7] In 2010, Perruchas *et al.* reported the mechanochromic properties of a tetranuclear cubane-type Cu(I) iodide cluster $[Cu_4I_4(PPh_2(CH_2CH = CH_2))_4]$, whose emission color dramatically changed from pale green to yellow after grinding, and the initial emission color was fully recovered by exposure to volatile solvent or heating.[8] These Cu_nI_n (n = 4, 6, 8, and so on) clusters (Fig. 1a) represent the most common type of Cu(I)-based MCL material.[9] In addition, several Cu(I)-based coordination polymers (Fig. 1b), which are metal–organic frameworks, also possess MCL properties.[10]

Although cuprophilic interaction is considered as essential to MCL, some studies have challenged the dominant view. For example, Yang *et al.* reported a mechanochromic phenomenon in a cubane Cu_4I_4 cluster without Cu–Cu interaction.[11] It is worth noting that Steffen *et al.* studied four ionic Cu(I)–NHC complexes, and proposed a new mechanism for the cation–anion exciplex.[12] In

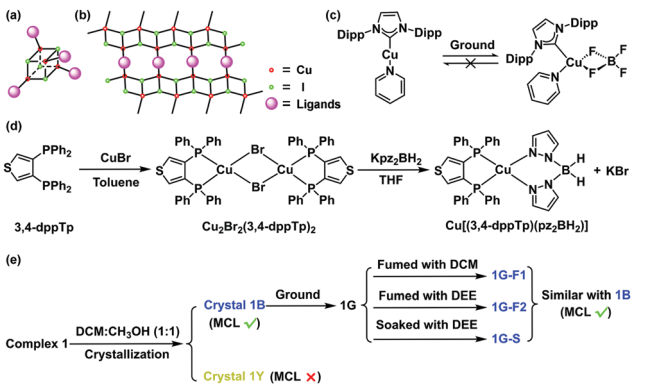

Fig. 1 (a) A tetranuclear cubane-type Cu(I) iodide cluster with MCL properties. (b) A Cu(I)-based coordination polymer with MCL properties. (c) Linear mononuclear Cu(I)–NHC complexes. (d) The synthetic route to the title complex Cu[(3,4-dppTp)(pz_2BH_2)] (**1**). (e) The relationship between the various forms of complex **1**. DCM and DEE are the abbreviations for dichloromethane and diethyl ether, respectively.

[a] *Department of Chemistry, Capital Normal University, Beijing, 100048, China. E-mail: jinqh@mail.cnu.edu.cn*
[b] *Beijing National Laboratory for Molecular Sciences (BNLMS), State Key Laboratory of Rare Earth Materials Chemistry and Applications, Beijing Engineering Technology Research Centre of Active Display, College of Chemistry and Molecular Engineering, Peking University, Beijing, 100871, China. E-mail: zwliu@pku.edu.cn*

† Electronic supplementary information (ESI) available: Experimental section, characterization, and physical measurements. CCDC 2051659 and 2063940. For ESI and crystallographic data in CIF or other electronic format see DOI: 10.1039/d1cc01229k

This journal is © The Royal Society of Chemistry 2021

Published on 13 April 2021. Downloaded on 4/5/2026 1:25:58 AM.

2019, Steffen and co-workers synthesized some linear mononuclear Cu(I)–NHC complexes (Fig. 1c) that exhibited significant changes in their photophysical properties after grinding.[13] This phenomenon was also caused by the Cu–F interaction formed during the grinding process. Unfortunately, these ground Cu(I)–NHC compounds cannot return to their initial photoluminescence color.

Very recently, Chen and co-workers reported a series of multinuclear Cu(I) complexes exhibiting MCL properties, which was due to π···π or N–H···O hydrogen bonds.[14] However, to our knowledge, mononuclear Cu(I) complexes with reversible MCL properties have not yet been reported. Obviously, the crowded environment around the center metal in mononuclear Cu(I) complexes usually leads to sufficiently long Cu–Cu distances that can eliminate the Cu–Cu interactions, and research on such materials can provide new perspectives on MCL mechanisms.

Introducing flexible fragments to promote the formation of a loose crystal structure is considered as a useful strategy to achieve MCL molecules.[4] However, bright luminescence Cu(I) complexes are usually obtained by employing ligands with greater steric rigidity to suppress the pseudo-Jahn–Teller distortion and other non-radiative decay of the excited states.[6a] To solve this dilemma, we selected the anionic ligand bis(pyrazol-1-yl)borohydrate, *i.e.*, pz_2BH_2, which is a relatively flexible but efficient ligand that can be used to construct luminescent Cu(I) complexes.[15] In addition, a rigid ligand 3,4-bis(diphenyl phosphino)thiophene (3,4-dppTp) was also employed to suppress the flattening process. Utilizing the two specific ligands, a mononuclear neutral Cu(I) complex Cu[(3,4-dppTp)(pz_2BH_2)] (**1**) was obtained. The synthetic route to complex **1** is shown in Fig. 1d. The final product was fully characterized by ^1H (^{13}C, ^{31}P) NMR spectroscopy, mass spectrometry, and elemental analysis. Detailed procedures and characterization information are presented in the Supporting Information. In addition, we obtained two crystals of complex **1**. As expected, the blue emissive crystals showed evident MCL properties with emission color variation between blue and yellow.

The two different forms of complex **1** are named **1B** and **1Y**, where the letter denotes its emission color (B denotes blue, and Y denotes yellow-green). The two crystals were characterized by single crystal X-ray diffraction (SCXRD, Table S1, ESI†). According to the UV-Vis absorption spectra (Fig. S10, ESI†), the intense absorption bands with maxima of 250 nm and 295 nm were assigned to the spin-allowed π–π* transitions of the 3,4-dppTp ligand. The transition of pz_2BH_2 was expected to occur at shorter wavelengths. At a longer wavelength, complex **1** exhibited a weak absorption shoulder peak that was attributed to d–π* transitions.

These analyses are supported by density functional theory (DFT) calculations. In alignment with most Cu(I) complexes,[6a] compound **1** exhibited metal to ligand charge transfer (MLCT) excited characteristics, where the highest occupied molecular orbital (HOMO) was mainly distributed around Cu(I), and the lowest unoccupied molecular orbital (LUMO) mainly resided on the π orbitals of the central thiophene rings (Fig. S11, ESI†).

Under UV excitation, the two polymorphs exhibited bright blue and yellow-green luminescence, and their maximum emission wavelength (λ_{max}) was 472 nm to 528 nm, respectively.

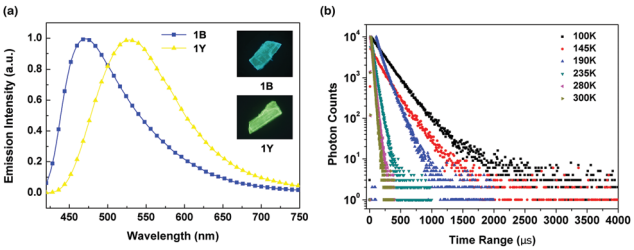

Fig. 2 (a) Photoluminescence spectra of the two crystal forms at room temperature; inset: photographs of **1B** and **1Y** under UV light (365 nm). (b) Temperature-dependent photoluminescence spectra of **1B**.

Their photoluminescence absolute quantum yield (Φ_{PL}) was 59% and 78%, and the excited state decay lifetime (τ) was 22 μs and 19 μs, respectively (Fig. 2 and Table 1). Based on the equations $k_r = \Phi_{PL}/\tau$ and $\Phi_{PL} = k_r/(k_r + k_{nr})$,[16] where k_r and k_{nr} denote the radiative constant and non-radiative constant, respectively, the crystal form **1Y** exhibited a higher k_r but a k_{nr} that was lower than **1B**, indicating a more rigid coordination environment around the Cu(I) centers. Additionally, the temperature-dependent photoluminescence spectra and the excited state lifetimes (Fig. 2b, Fig. S12–S17 and Table S3, ESI†) of **1B** and **1Y** were examined. It was observed that the complex exhibited a thermally activated delay fluorescence (TADF) mechanism.

Interestingly, the blue emission polymorph **1B** exhibited evident MCL properties, while the yellow-green emission polymorph **1Y** did not. For **1B**, the colorless crystal became a yellow powder **1G** upon grinding, and the λ_{max} displayed a remarkable redshift of approximately 80 nm, accompanied by an emission color variation from blue to yellow (Fig. 3 and Table 1). The blue luminescence was completely regained by fuming **1G** to dichloromethane (**1G-F1**) or diethyl ether vapors (**1G-F2**), and it was also recovered by soaking **1G** in diethyl ether (**1G-S**). Note that this ground-fumed conversion can only be performed three times, while the ground-soaked conversion showed no degradation even after ten cycles.

To understand the MCL phenomenon, detailed photophysical properties of the various states of **1B** during the ground-fumed/soaked conversion, *i.e.*, **1G**, **1G-F1**, **1G-F2**, and **1G-S** were measured (Fig. 3b, c and Table 1). In addition, a neat film of complex **1** (**1-Film**) was prepared by spin-coating and was characterized for comparison. The ground sample **1G**

Table 1 Photophysical data for complex **1** in the two crystal forms, as a neat film, and in various states during the ground-fumed/soaking conversion

	λ_{max} [nm]	Φ_{PL}[a] [%]	τ [μs]	k_r [10^4 s^{-1}]	k_{nr} [10^4 s^{-1}]	CIE (x, y)
1B	472	59	22	2.68	1.86	(0.22, 0.30)
1Y	528	78	19	4.11	1.16	(0.34, 0.51)
1G	550	34	15	2.27	4.41	(0.40, 0.52)
1G-F1	469	36	20	1.80	3.20	(0.19, 0.26)
1G-F2	478	61	22	2.77	1.77	(0.23, 0.34)
1G-S	469	58	19	3.05	2.21	(0.19, 0.25)
1-Film	554	10	7	1.43	12.87	(0.41, 0.51)

[a] Absolute quantum yields determined using an integrating sphere.

Published on 13 April 2021. Downloaded on 4/5/2026 1:25:58 AM.

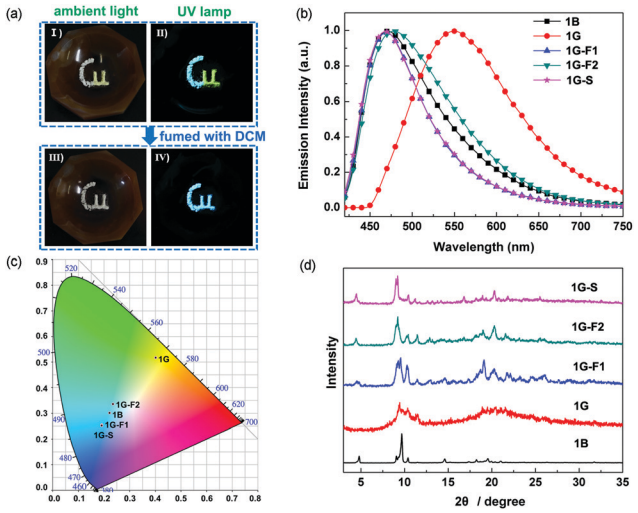

Fig. 3 (a) Photos of various states of **1B** during the ground-fumed conversion. Photos I and III were taken under ambient light, while photos II and IV were taken under a UV lamp (365 nm). In photos I and II, the letters "C" and "u" are made up of 1B and 1G samples, respectively. Photos III and IV show the state after fumigation with DCM, where the luminescent color of the letter "u" changed from yellow to blue. (b) Photoluminescence spectra of various states of **1B** during the ground-fumed/soaking conversion. (c) The CIE 1931 chromaticity diagram of various states of **1B** during the ground-fumed/soaked conversion. It should be noted that the coordinate points of **1G-F1** and **1G-S** are almost coincident. (d) Powder X-ray diffraction (PXRD) spectra of the various states of **1B** during the ground-fumed/soaked conversion.

showed an almost identical emission spectrum to that of **1-Film** (Fig. S18, ESI†), indicating that the coordination environment of Cu(I) complexes in the ground sample was similar to that in the amorphous film. A comparison of **1G** with **1B** indicated an obvious decrease in Φ_{PL} (Table 1), which may arise from the less rigid environment in amorphous **1G** than that in crystal **1B**, leading to increased non-radiative transitions. The difference in Φ_{PL} between **1G** and **1-Film** was also caused by environmental rigidity. In previous studies on Cu(I) complexes, there are often large differences in the Φ_{PL} values for powder and neat film.[13,17] Although the blue emission could be recovered in **1G-F1**, **1G-F2**, and **1G-S**, there were minute differences between the emission spectra for these samples, but obvious differences in Φ_{PL}. Based on the deduced k_r and k_{nr} values, the higher Φ_{PL} mainly arises from the lower non-radiative rate.

In addition, the powder X-ray diffraction (PXRD) spectra for the various states of **1B** during the ground-fumed/soaked conversion were also measured to understand the MCL phenomenon (Fig. 3d). Sample **1B** exhibited intense and sharp diffraction peaks, while the peaks of **1G** become very broad, indicating the crystal-to-amorphous phase transition upon grinding.[5c,18] After exposing **1G** to solvent vapors or soaking in diethyl ether, intense characteristic signals were observed once more. The PXRD patterns of **1G-F1** and **1G-F2** were somewhat different from the pattern of **1B**, while the pattern of **1G-S** was very similar to **1B**, illustrating that recrystallization was more complete in the ground-soaked conversion.

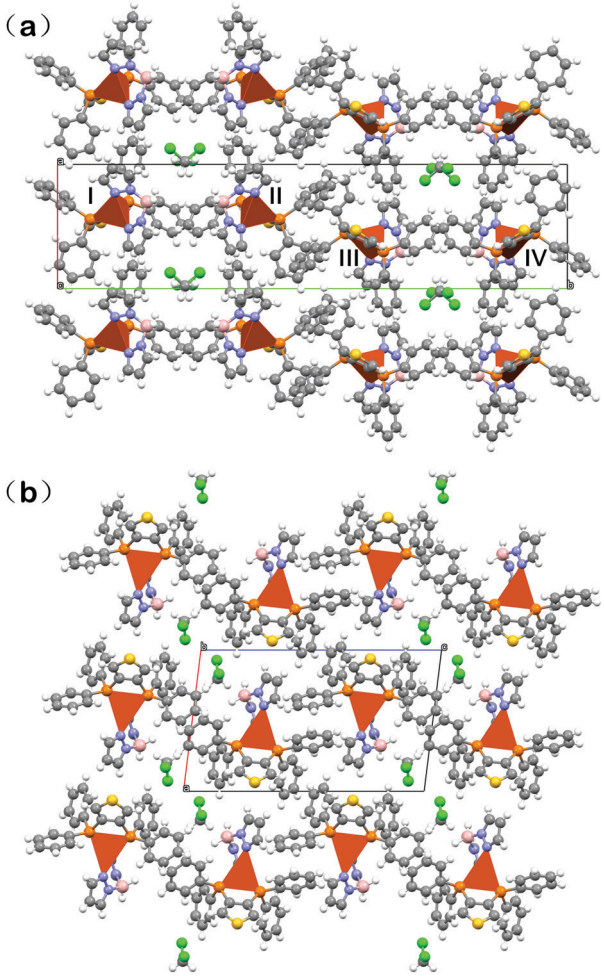

Fig. 4 A molecular packing comparison of (a) **1B** viewed down the *c*-axis showing the pore structure and (b) **1Y** viewed down the *b*-axis. Atom notation: B, pink; C, grey; Cl, green; Cu, red; H, white; N, blue; P, orange; and S, yellow.

To explore the underlying mechanism of this MCL phenomenon, packing modes and intermolecular forces of the two crystal forms were investigated in detail. In terms of **1B**, there are four molecules (numbered as I–IV, Fig. 4a) interlaced along the *b*-axis in each unit cell. Among which, molecules II and III are connected to each other by a C–H···π bond (2.931 Å, Fig. S19, ESI†), and they tightly interact with molecules in adjacent unit cells by two types of C–H···π bonds (2.663 and 2.895 Å). Between I and II (or III and IV), there is a pore along the *c*-axis that is filled with alternately arranged dichloromethane molecules. These solvent molecules are connected to each other by C–H···Cl bonds (2.837 Å). In addition, these dichloromethane molecules also act as glue, linking molecules I and II (or III and IV) through C–H···Cl bonds (3.084 and 3.087 Å). Rich intermolecular forces are also found in **1Y** (Fig. S20, ESI†). It contain two C–H...π bonds (2.754 Å and 2.840 Å), two types of B–H···H–C dihydrogen bonds (2.201 Å, 167.90° and 2.322 Å, 176.13°), one C–H···Cl bond (3.098 Å) and one C–H···N bond (2.587 Å). Obviously, the intermolecular force becomes stronger, but the role of solvent molecules in **1B** is impaired. The solvent no longer

 This journal is © The Royal Society of Chemistry 2021

Published on 13 April 2021. Downloaded on 4/5/2026 1:25:58 AM.

acts as a glue to link complex molecules, and no pore structure was observed in it.

As shown in Fig. S21 (ESI†), there are no changes in the ^{1}H NMR spectroscopy of **1B**, **1G**, and **1G-F1** except for the solvent peak of dichloromethane. This suggests that there are no changes in the coordination modes during the ground-fumed process. Furthermore, the infrared spectra (Fig. S22, ESI†) were measured to support this conclusion. There are no shifts of the absorption peaks, which confirms that the coordination mode has not changed. However, some peaks between 3000 and 3150 cm^{-1} (corresponding to the stretching of C–H bonds) almost disappeared after grinding. This phenomenon is related to the change in the intramolecular or intermolecular interactions,[3e,14a] indicating that the packing mode has changed. This is consistent with the conclusion obtained by PXRD. In addition, the minimum Cu–Cu distance in **1B** is 9.392 Å (Fig. S23, ESI†), which is much longer than the sum of van der Waals radii (2.80 Å). Therefore, the pore structure is proposed to rationalize their MCL properties. The unique pore structure is caused by a variety of non-covalent interactions. The use of grinding or fuming and soaking to break or reconstruct the pore structure, *i.e.*, tuning the weak interactions, significantly changes the bond lengths and angles of Cu(I) complexes, resulting in differences in their luminescence colors.

In summary, a novel mononuclear Cu(I) complex was designed, and two polymorphs exhibiting different color emission were isolated. Interestingly, the blue-luminescent crystals have evident MCL properties, with the emission color varying between blue and yellow upon grinding and fuming/soaking. The MCL phenomenon, which was first observed in mononuclear Cu(I) complexes, was studied in detail. Based on photophysical and structural analysis, the pore structure existing in the blue emission crystals provides a flexible space so that external force can easily change the coordination environment of the central Cu(I) atom, leading to a drastic emission color change to yellow. These results demonstrate that mononuclear Cu(I) complexes could be promising but unexplored MCL materials.

We gratefully acknowledge financial support from the National Key R&D Program of China (2017YFA0205100, 2016YFB0401001) and the Beijing Natural Science Foundation (No. 2172017).

Conflicts of interest

There are no conflicts of interest to report.

Notes and references

1 (*a*) A. J. McConnell, C. S. Wood, P. P. Neelakandan and J. R. Nitschke, *Chem. Rev.*, 2015, **115**, 7729–7793; (*b*) J. Ochi, K. Tanaka and Y. Chujo, *Angew. Chem., Int. Ed.*, 2020, **59**, 2699–2710.
2 (*a*) Y. Sagara and T. Kato, *Nat. Chem.*, 2009, **1**, 605–610; (*b*) O. S. Wenger, *Chem. Rev.*, 2013, **113**, 3686–3733; (*c*) B. Li, H. T. Fan, S. Q. Zang, H. Y. Li and L. Y. Wang, *Coord. Chem. Rev.*, 2018, **377**, 307–329; (*d*) C. M. Brown, V. Carta and M. O. Wolf, *Chem. Mater.*, 2018, **30**, 5786–5795.
3 (*a*) S. J. Yoon, J. W. Chung, J. Gierschner, K. S. Kim, M. G. Choi, D. Kim and S. Y. Park, *J. Am. Chem. Soc.*, 2010, **132**, 13675–13683; (*b*) D. Genovese, A. Aliprandi, E. A. Prasetyanto, M. Mauro, M. Hirtz, H. Fuchs, Y. Fujita, H. Uji-I, S. Lebedkin, M. Kappes and L. De Cola, *Adv. Funct. Mater.*, 2016, **26**, 5271–5278; (*c*) L. Liu, X. Wang, N. Wang, T. Peng and S. Wang, *Angew. Chem., Int. Ed.*, 2017, **56**, 9160–9164; (*d*) Y. Yang, X. Yang, X. Fang, K. Z. Wang and D. Yan, *Adv. Sci.*, 2018, **5**, 1801187; (*e*) G. Huang, Y. Jiang, S. Yang, B. S. Li and B. Z. Tang, *Adv. Funct. Mater.*, 2019, **29**, 1900516; (*f*) Y. Liu, A. Li, S. Xu, W. Xu, Y. Liu, W. Tian and B. Xu, *Angew. Chem., Int. Ed.*, 2020, **59**, 15098–15103.
4 Y. Sagara, S. Yamane, M. Mitani, C. Weder and T. Kato, *Adv. Mater.*, 2016, **28**, 1073–1095.
5 (*a*) Y. A. Lee and R. Eisenberg, *J. Am. Chem. Soc.*, 2003, **125**, 7778–7779; (*b*) H. Ito, M. Muromoto, S. Kurenuma, S. Ishizaka, N. Kitamura, H. Sato and T. Seki, *Nat. Commun.*, 2013, **4**, 2009; (*c*) N. M. Wu, M. Ng and V. W. Yam, *Angew. Chem., Int. Ed.*, 2019, **58**, 3027–3031.
6 (*a*) Y. Zhang, M. Schulz, M. Wächtler, M. Karnahl and B. Dietzek, *Coord. Chem. Rev.*, 2018, **356**, 127–146; (*b*) R. Hamze, J. L. Peltier, D. Sylvinson, M. Jung, J. Cardenas, R. Haiges, M. Soleilhavoup, R. Jazzar, P. I. Djurovich, G. Bertrand and M. E. Thompson, *Science*, 2019, **363**, 601–606.
7 E. Cariati, E. Lucenti, C. Botta, U. Giovanella, D. Marinotto and S. Righetto, *Coord. Chem. Rev.*, 2016, **306**, 566–614.
8 S. Perruchas, X. F. Le Goff, S. Maron, I. Maurin, F. Guillen, A. Garcia, T. Gacoin and J. P. Boilot, *J. Am. Chem. Soc.*, 2010, **132**, 10967–10969.
9 (*a*) X. C. Shan, F. L. Jiang, L. Chen, M. Y. Wu, J. Pan, X. Y. Wan and M. C. Hong, *J. Mater. Chem. C*, 2013, **1**, 4339; (*b*) Q. Benito, X. F. Le Goff, S. Maron, A. Fargues, A. Garcia, C. Martineau, F. Taulelle, S. Kahlal, T. Gacoin, J. P. Boilot and S. Perruchas, *J. Am. Chem. Soc.*, 2014, **136**, 11311–11320; (*c*) Q. Benito, I. Maurin, T. Cheisson, G. Nocton, A. Fargues, A. Garcia, C. Martineau, T. Gacoin, J. P. Boilot and S. Perruchas, *Chem. – Eur. J.*, 2015, **21**, 5892–5897.
10 (*a*) T. Wen, D. X. Zhang, J. Liu, R. Lin and J. Zhang, *Chem. Commun.*, 2013, **49**, 5660–5662; (*b*) T. Wen, X. P. Zhou, D. X. Zhang and D. Li, *Chem. – Eur. J.*, 2014, **20**, 644–648; (*c*) E. Kwon, J. Kim, K. Y. Lee and T. H. Kim, *Inorg. Chem.*, 2017, **56**, 943–949; (*d*) J. Conesa-Egea, J. Gallardo-Martinez, S. Delgado, J. I. Martinez, J. Gonzalez-Platas, V. Fernandez-Moreira, U. R. Rodriguez-Mendoza, P. Ocon, F. Zamora and P. Amo-Ochoa, *Small*, 2017, **13**, 1700965.
11 K. Yang, S. L. Li, F. Q. Zhang and X. M. Zhang, *Inorg. Chem.*, 2016, **55**, 7323–7325.
12 B. Hupp, J. Nitsch, T. Schmitt, R. Bertermann, K. Edkins, F. Hirsch, I. Fischer, M. Auth, A. Sperlich and A. Steffen, *Angew. Chem., Int. Ed.*, 2018, **57**, 13671–13675.
13 A. Liske, L. Wallbaum, T. Hölzel, J. Föller, M. Gernert, B. Hupp, C. Ganter, M. C. Marian and A. Steffen, *Inorg. Chem.*, 2019, **58**, 5433–5445.
14 (*a*) D. Peng, L. H. He, P. Ju, J. L. Chen, H. Y. Ye, J. Y. Wang, S. J. Liu and H. R. Wen, *Inorg. Chem.*, 2020, **59**, 17213–17223; (*b*) X. W. Chen, L. H. He, P. Ju, J. L. Chen, S. J. Liu and H. R. Wen, *J. Mater. Chem. C*, 2020, **8**, 16160–16167.
15 (*a*) R. Czerwieniec, J. Yu and H. Yersin, *Inorg. Chem.*, 2011, **50**, 8293–8301; (*b*) R. Czerwieniec, J. Yu and H. Yersin, *Inorg. Chem.*, 2012, **51**, 1975.
16 T. Sajoto, P. I. Djurovich, A. Tamayo, M. Yousufuddin, R. Bau, M. E. Thompson, R. J. Holmes and S. R. Forrest, *Inorg. Chem.*, 2005, **44**, 7992–8003.
17 D. M. Zink, D. Volz, T. Baumann, M. Mydlak, H. Flügge, J. Friedrichs, M. Nieger and S. Bräse, *Chem. Mater.*, 2013, **25**, 4471–4486.
18 T. T. Lu, J. Y. Wang, D. S. Tu, Z. N. Chen, X. T. Chen and Z. L. Xue, *Inorg. Chem.*, 2018, **57**, 13618–13630.